# Rearrangement of topological defects and anchoring on the inclusion boundary in ferroelectric smectic membranes

P. V. Dolganov,[1] H. T. Nguyen,[2] E. I. Kats,[3] V. K. Dolganov,[1] and P. Cluzeau[2]
[1]*Institute of Solid State Physics, Russian Academy of Sciences, 142432, Chernogolovka, Moscow district, Russia*
[2]*Centre de Recherche Paul Pascal, CNRS, Avenue A. Schweitzer, 33600 Pessac, France*
[3]*Laue-Langevin Institute, F-38042, Grenoble, France*
*and L.D. Landau Institute for Theoretical Physics, RAS, 117940 GSP-1, Moscow, Russia*
(Received 17 November 2006; published 15 March 2007)

We report experiments on a ferroelectric membrane and droplets with tunable surface properties. In smectic membranes the configuration of the **c**-director field near inclusions may be rearranged drastically with temperature. The transformation of the **c**-director field results from the competition between the elastic and polar properties of the membranes. We demonstrate that anchoring conditions on the inclusion boundary are not fixed but depend on the temperature. A dipolar **c**-director configuration near droplets can evolve to a mixed configuration and to a quadrupolar one. These modifications of the **c**-director field near the inclusions lead to a change of the interaction between the inclusions, their self-organization, and even to the destruction of structures already formed by the inclusions. Our observations open new possibilities for manipulating inclusions and controlling their self-organization.

DOI: 10.1103/PhysRevE.75.031706 PACS number(s): 61.30.Jf, 61.30.Gd, 81.16.Dn

## I. INTRODUCTION

Liquid crystals and inclusions may form self-organizing emulsions with unusual structures and properties [1–5]. Formation of ordered structures from inclusions occurs due to unique properties of liquid crystals, namely, the orientational anisotropy and fluidity. Inclusions deform the field of molecular ordering of the liquid-crystal medium. The deformation induced by the inclusions may partially relax via an appropriate orientation of inclusions and their mutual position. This mechanism of interaction and self-organization leads to the formation of various structures with a fixed distance between the inclusions and their orientation. Ordered structures from inclusions were found in nematic [1–5], smectic [6–12] liquid crystals, the liquid crystal-air interface [13]. The greatest diversity of different structures was found in smectic membranes: linear chains [6–10,12], clusters [7,12], hexagonal [8,9] and square [7–9] two-dimensional (2D) structures with translational ordering. In membranes 2D emulsions from droplets can be formed by heating the membrane above the melting temperature of the smectic phase in the bulk sample.

Membranes of smectic liquid crystals can be prepared with thickness from two to several thousand layers. The layer planes are parallel to the free surfaces [14,15]. In the smectic-*C*-type liquid crystals every layer is a 2D oriented liquid with nematic director **n** tilted with respect to the layer normal. Projections of **n** on the layer plane form a 2D field of molecular ordering or **c**-director field [16]. The tilted smectic *C* phase has a mirror symmetry plane, perpendicular to the layers and a twofold rotation symmetry axis in the direction normal to the tilt plane. If the layer normal points along the *Z* axis, and the twofold symmetry axis is taken to be the *X* axis, then the corresponding symmetry operations are $X \rightarrow -X$ (plane of symmetry) and $Y,Z \rightarrow -Y,-Z$ (twofold rotation). As a result of the invariance with respect to these transformations the smectic *C* structure is also invariant with respect to change of handedness of the *XYZ* frame, i.e., achiral. In the case under consideration of the chiral ferroelectric smectic $C^*$ (Sm$C^*$) phase, the mirror symmetry is broken.

The long-range interaction between the inclusions [17,18] originates from the elastic deformation of the **c**-director induced by the inclusions. Such deformation is associated with the **c**-director orientation defined by director anchoring on the inclusion boundary. The most interesting situation appears when anchoring conditions (tangential or radial) are strong. Such inclusions are equivalent to point topological defects with topological charge $S=+1$. The conservation of the topological charge in the system requires that the formation of inclusions in a defect-free film is accompanied by nucleation of topological defect(s) with total topological charge $S=-1$. It is essential that at the same boundary conditions various types of topological defects, which could be localized in different places, may exist. It is the localization of topological defect(s) near the inclusions that mainly determines the anisotropy, the strength of the interparticle interaction, and the assembly of inclusions. In 2D smectic liquid-crystalline layers, pointlike defects with integer charges are topologically stable. Half-integer charge defects can exist only attached to an interface because the **c**-director is a polar vector.

Up to now transformation of topological defects and configuration of the director field has been observed only in nematic liquid crystals (note also the recent publication [19] reporting on textural transformations in islands on freestanding Sm$C^*$ films). Transformation of the director field was detected upon changing the inclusion size [2,20–24]. Near a small inclusion the symmetry of the director field is quadrupolar with a ringlike topological defect near the inclusion ("Saturn ring"). On increasing the inclusion size the Saturn ring transforms into a point topological defect. The configuration of the director field becomes dipolar. A very recent paper by Völtz *et al.* [25] reports a direct observation of the

 ©2007 The American Physical Society

transformation from a point defect (hyperbolic hedgehog) to a Saturn ring when the size of the gas bubble in the nematic liquid crystal is decreased by applied pressure. This transformation was explained from the energetical point of view: the energy of the linear defect increases with its size and the Saturn ring becomes unstable with respect to the configuration with the point defect.

In smectic membranes both dipolar [6,10] and quadrupolar [7,8] configurations of the **c**-director were observed in different materials. A widely accepted view is that the **c**-director configuration and interaction between inclusions is constant for a given membrane and inclusion.

We present here experimental evidence, and a heuristic theoretical description for topological transitions between dipolar, mixed, and quadrupolar symmetry configurations of the **c**-director around the droplets. We find a dramatic transformation of the director configuration near inclusions (cholesteric droplets) in Sm$C^*$ membranes. Up to now, it was thought that the **c**-director configuration near the inclusions, their interaction, and self-organization are determined by the elasticity of the media. Our results highlight that in ferroelectric membranes the polarity of the membrane is also essential for the inclusion behavior. The competition between elastic and polar properties leads to the transformation of the **c**-director field, the position of the topological defect(s) on the inclusion boundary, and even the number of defects and their strength. These transformations can be controlled by external conditions, e.g., temperature. The droplet can reversibly change the surface orientation of the **c**-director. The formation of structures from inclusions, their dissociation, and the subsequent formation of new structures are observed along with transformation of the **c**-director field near inclusions.

## II. EXPERIMENTAL SETUP

The experiments were carried out on membranes of chiral *S*-4′-nonyloxybiphenyl-4-yl 4-(1-methylheptyloxy)benzoate (9BSMHOB) and *S*-4′-undecyloxybiphenyl-4-yl 4-(1-methylheptyloxy)benzoate (11BSMHOB) [26]. The substances have the following phase sequences: K-(56.8 °C)-Sm$C^*$-(104.6C)-$N^*$-(131.4 °C)-I (9BSMHOB) and K-(56.5 °C)-Sm$C^*$-(106.4 °C)-$N^*$-(123.9 °C)-I (11BSMHOB). Membranes were prepared by drawing a small amount of the material in the Sm$C^*$ state across a 3 mm hole in a glass plate. The droplets and textures of the membrane were observed with an optical microscope in reflection mode. Observations between crossed polarizers (PRLM) and in depolarized light-reflected microscopy (DRLM) [27] were performed. Images were taken with a CCD camera. Cholesteric droplets were created in the membrane by heating the membrane above the bulk Sm$C^*$-$N^*$ transition temperature $T_C$. Part of the measurements were made with membranes in which the **c**-director was oriented by the electric field applied in the membrane plane. The electric field was used to determine the orientation of the droplet-defect pairs in membranes. Note that the electric field did not influence the transformation of droplet-defect pairs.

## III. EXPERIMENTAL RESULTS

In smectic membranes the droplets nucleate at certain temperatures directly related to thinning transition temperatures when the number of smectic layers $N$ in the membrane decreases [28]. The first droplet nucleation occurs right above the bulk transition temperature. These droplets are preserved in the membrane up to the temperature of thinning transition. The thinning front as a rule drags most of the droplets and carries them to the membrane meniscus. So after thinning the membrane remains free from droplets or with only a small number of them. On further heating in a certain temperature interval droplets do not nucleate. Nucleation may occur at temperatures somewhat lower than the temperature of the next thinning transition $T_N$. These droplets exist within the temperature interval from $T_C$ to $T_N$. Upon heating the next thinning transition and the next droplet nucleation can be observed. Notice that the temperature interval of droplet existence increases upon decreasing the membrane thickness. The droplet formation can be crudely understood following the well-known fact that across a flat liquid interface in equilibrium no pressure difference can exist. This is not true anymore for smectic surface because the layers are elastic and therefore can support a normal stress that will equilibrate a pressure difference $\Delta P$ (of course if the latter one is not too large). In addition to the surface tension $\gamma$ this pressure difference contributes also to the tension $\Gamma$ along the smectic membrane

$$\Gamma = 2\gamma + \Delta P N d, \tag{1}$$

where $d$ is the layer thickness. The thickness of smectic membranes can be modified by nucleation of edge-dislocation loops (thinning transition decreases $\Gamma$). Another possibility is to modify both the material parameters ($\Gamma$ and $\gamma$) by a surface phase transition (Sm$C^*$-$N^*$ in our case). If due to temperature increase the smectic layering disappears, it cannot support the pressure difference $\Delta P$ anymore and cholesteric droplets in the membrane can be stabilized in a certain window of the parameters. Droplets in the membranes nucleate along with point topological defect $S=-1$ on the droplet boundary [Fig. 1(a)]. The configuration of the **c**-director field is dipolar. At low temperature the orientation of the **c**-director on the droplet boundary is planar [29]. The **c**-director configuration near the droplet is shown in Fig. 2(a). The polar axis connecting the droplet center and the defect orients perpendicular to the **c**-director far field. Dipole-dipole attraction leads to the formation of chains from droplets [Fig. 1(b)]. In membranes with the oriented **c**-director in all nucleated droplets the defects localize on the same side of droplets [Fig. 1(c)]. However, this position does not remain the same with temperature. Below we shall describe and discuss droplet behavior and the transformation of the director field when the orientation of the **c**-director on the droplet boundary remains planar (Sec. III A) and changes from planar to radial (Sec. III B).

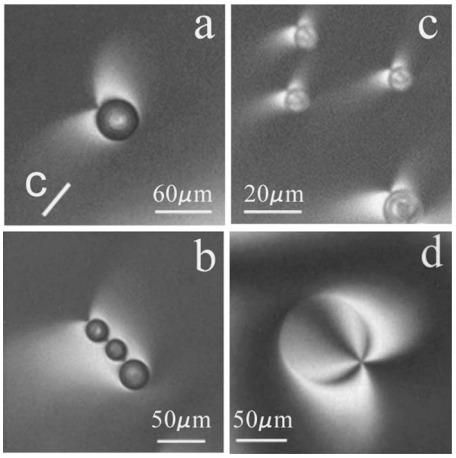


FIG. 1. A droplet-defect pair (a) and a chain of droplets (b) in 9BSMHOB smectic membranes. Accompanying topological defects localize on the droplet boundary. In the membrane with the oriented **c**-director field (c) all defects localize on the same side of the droplets. (d) A smectic island with the planar **c**-director orientation on the island boundary. The line in (a) shows the **c**-director orientation in the black regions.

### A. Transformation of the c-director configuration near the droplets and chains with conservation of the tangential anchoring on the droplet boundary

In thick membranes the transformation of the topological defect on the droplet boundary and the **c**-director field were found near $T_C$. Tangential orientation of the **c**-director on the inclusion boundary was observed in smectic islands [Fig. 1(d)] and in droplets just above $T_C$. However, the reorientation of the droplet-defect pair takes place (Fig. 3) at a temperature $T_R$ slightly higher than $T_C$ ($T_R \sim T_C + 0.2\ ^\circ\mathrm{C}$). The topological defect with charge $S=-1$ on the droplet boundary [Fig. 3(a)] splits into two topological defects $S=-1/2$, which move in opposite directions along the droplet boundary [Figs. 3(b) and 3(c)]. During this motion the defects turn the **c**-director by 180° on the droplet boundary. The defects join on the opposite side of the droplet and again form a dipolar droplet-defect pair with $S=-1$ topological defect [Fig. 3(d)]. The motion of defects is accompanied by a reorientation of the **c**-director near the inclusion. The **c**-director configurations are shown in Fig. 2 for the droplet before (a), after (c) the reorientation, and in an intermediate state (b). The force lines of the **c**-director field (Fig. 2) have been calculated using the electromagnetic analogy [17,29]. The droplet-defect pair is characterized by the topological dipole moment $\mathbf{p}=\Sigma \mathbf{r}_i S_i$, where $\mathbf{r}_i$ are the positions and $S_i$ are the charges of the physical and virtual topological defects [17]. In the reorientation process the dipolar moment of the droplet-defect pair decreases, reaches zero (the droplet in Fig. 3(c) with quadrupolar configuration), and then again forms a dipolar configuration with the opposite direction of the topological dipole moment. In the membranes oriented by the electric field the topological dipole at high temperature orients in the direction of the field. At low temperature the topological dipole orients in the direction opposite to the direction of the electric field. The reorientation is reversible and occurs both on heating and on cooling.

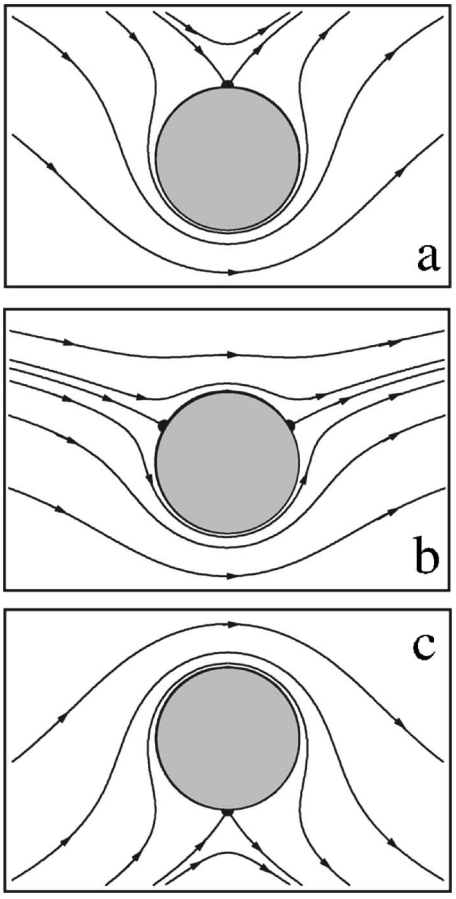


FIG. 2. The **c**-director configuration near a dipolar droplet with planar boundary conditions (a). The **c**-director field after the reorientation of the defect (c) and during the reorientation (b).

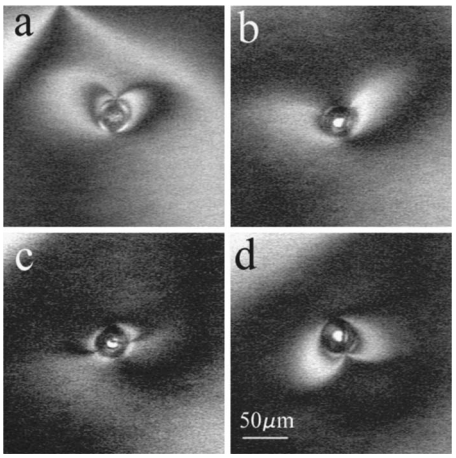


FIG. 3. Reorientation of the **c**-director field near the inclusion in thick membranes ($N>20$). (a) A droplet with dipolar configuration of the **c**-director field, $T=106.4\ ^\circ\mathrm{C}$. The membrane was heated [(b)–(d)]. The point topological defect $S=-1$ splits in two $S=-1/2$ defects (b) which move along the inclusion boundary and join on the other side of the inclusion forming again a topological defect with $S=-1$, $T=106.6\ ^\circ\mathrm{C}$ (d). During reorientation the **c**-director field passes through the quadrupolar configuration (c) (PRLM, 11BSMHOB).

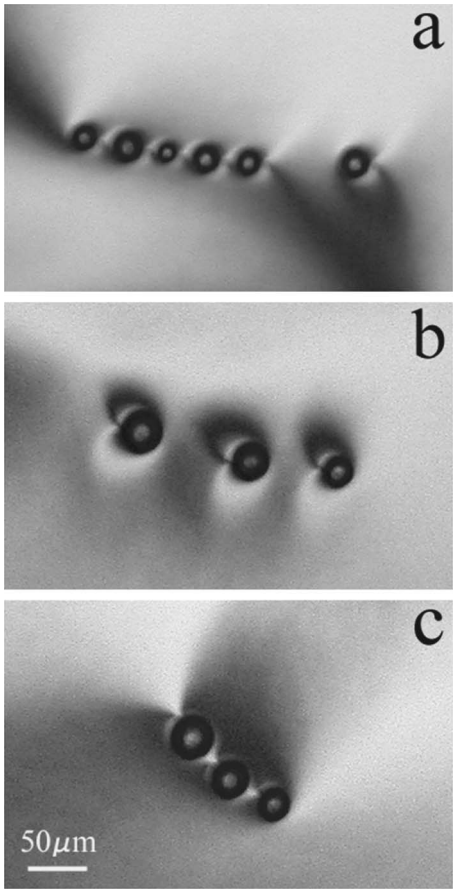


FIG. 4. Rearrangement of the **c**-director field near the droplets leads to the detachment of chains and the subsequent self-organization of droplets in new chains. (a) A chain and a single droplet in the membrane, $T=104.7$ °C. (b) At heating the **c**-director near the single droplet is reoriented [the right droplet in (a) and (b)]. The chain is broken and two right and three left droplets from the chain (a) coalesce forming two larger droplets [the left two droplets in (b)]. The interaction between the droplets with the new **c**-director configuration leads to the formation of a new chain, $T=105$ °C (c) (DRLM, 9BSMHOB).

The reorientation of director configuration leads to a dramatic change of the collective behavior of inclusions (Fig. 4). Figure 4(a) shows an individual droplet and a chain formed by five droplets at low temperature. On heating to the temperature $T_R$ [Fig. 4(b)] the reorientation of the **c**-director occurs not only around the individual droplet but also in the chain. In Fig. 4(b), the topological defects are already located on the opposite side of the droplets with respect to Fig. 4(a). During the reorientation the chain is destroyed, moreover, some droplets coalesce. The left droplet in Fig. 4(b) was formed from three left droplets of the chain in Fig. 4(a); the central droplet was formed by two right droplets from the chain in Fig. 4(a). The destruction of chains and the coalescence of droplets occur when surface $S=-1$ defects split into $S=-1/2$ defects and they move on the droplet boundary [Fig. 2(b)]. During such motion on the droplet boundary the short-range repulsion of droplets decreases, so they can approach each other and coalesce. After the formation of the new **c**-director configuration the attractive interaction organizes

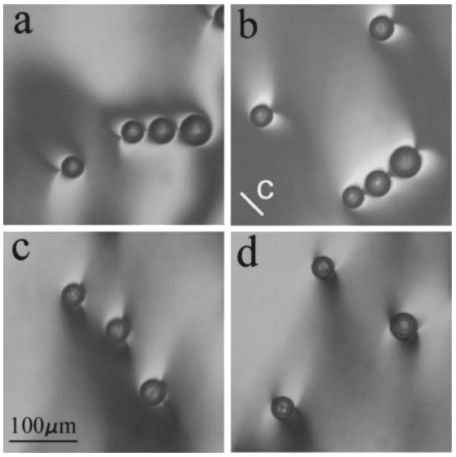


FIG. 5. The configuration of the **c**-director field near droplets and chains in membranes with $N<20$ essentially depends on temperature. At low temperature ($T=104.8$ °C) the dipolar configuration with a single boundary defect $S=-1$ is stable (a). At heating the topological defect $S=-1$ splits into two defects $S=-1/2$, $T=105.1$ °C (b). These defects localize on the opposite side of the droplet with respect to the initial state (a). After **c**-director reorientation three droplets [the chain in (a)] formed a new chain (b) but now with two topological defects ($S=-1/2$) on the boundary of each droplet. Further heating leads to increasing the distance between $S=-1/2$ defects, $T=105.4$ °C (c). For a large distance between the defects, the chains become unstable. At $T=105.5$ °C the droplet-defect pairs become dipolar (d) with a radial orientation of the **c**-director on the droplet boundary. The line in (b) indicates the **c**-director orientation in black regions. The photos were taken in DRLM (9BSMHOB).

new chains from droplets [Fig. 4(c)]. The formation of chains and their destruction may be repeated by successive heating and cooling of the membrane above and below $T_R$.

Modifications of droplet and chain behavior were observed with decreasing membrane thickness. The main changes in the membranes thinner than 20 smectic layers are the following: (a) **c**-director reorientation near the droplets occurs in a certain temperature interval $\Delta T_R$; (b) this interval $\Delta T_R$ increases and slightly shifts to higher temperature with decreasing membrane thickness; (c) a configuration with two surface $S=-1/2$ topological defects [Fig. 2(b)] becomes stable, and the location of the $S=-1/2$ defects on the droplet boundary can be regulated by temperature variations. Figure 5 illustrates the droplet and chain behavior in a membrane with thickness about 17 smectic layers. At low temperature the dipolar **c**-director configuration is observed near the droplets and chains [Fig. 5(a)]. Reorientation of the **c**-director field starts with splitting of the surface $S=-1$ defect in two $S=-1/2$ defects. They further move in opposite directions (clockwise and counterclockwise) along the droplet boundary. However, the surface defects $S=-1/2$ do not adjoin forming the $S=-1$ defect on the opposite side of the droplet. The defects $S=-1/2$ remain localized on a certain distance from each other [Fig. 5(b)]. This intermediate configuration between pure dipolar and quadrupolar ones with a well-defined distance between defects is stable at constant temperature. In chains the splitting of $S=-1$ surface defects is similar to the splitting near individual droplets [Fig. 5(b)].

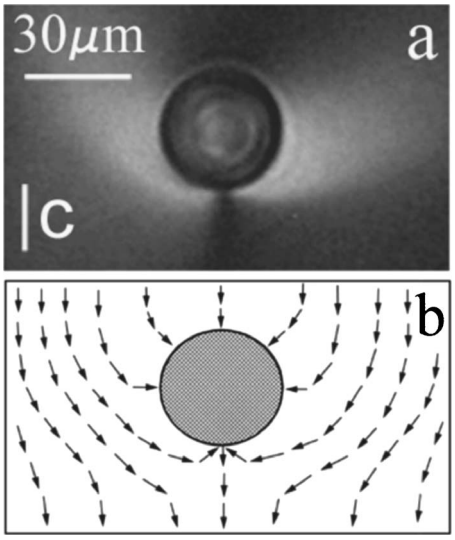


FIG. 6. A dipolar droplet with radial **c**-director orientation on the boundary of the droplet (a) and the schematic representation of the **c**-director field near the droplet (b). The dipole axis of the droplet orients parallel to the far-field **c**-director. The orientation of the **c**-director in black regions is vertical [the line in (a)] (DRLM, 9BSMHOB, $T=106.9$ °C).

Note that in the process of the **c**-director reorientation, the chains first disintegrate and then adjoin again. On further heating, the distance between surface defects may increase [Fig. 5(c)]. Modification of the location of $S=-1/2$ defects occurs in a temperature interval $\Delta T_R \sim 0.5$ °C. The angle between $S=-1/2$ defects becomes smaller in thinner membranes.

In summary, the reorientation described in this subsection is characterized by the following features: $S=-1$ topological defect splits into two $S=-1/2$ defects. They move along the droplet boundary and reorient the **c**-director by 180°. Surface orientation of the **c**-director remains planar. The complex transformation of the **c**-director configuration is reversible and is observed both on heating and on cooling.

### B. Transition from planar to radial orientation of the c-director on the droplet boundary

The transformation of droplets with accompanying defects continues at high temperature and leads to the formation of dipolar or quadrupolar configurations with radial anchoring. Droplets in Fig. 5(d) have radial **c**-director orientation on the droplet boundary. This orientation was formed from planar orientation [Fig. 5(c)] by a 90° rotation of the **c**-director on the droplet boundary. The texture and configuration of the **c**-director field near a dipolar droplet with radial anchoring are shown in Figs. 6(a) and 6(b). In the employed geometry of DRLM the **c**-director orientation in black regions is vertical. The dipole axis of the droplets orients parallel to the **c**-director far field. The droplets attract and form chains, which also orient parallel to the far-field **c**-director. We are Reminded that at low temperature the droplets and chains with planar anchoring orient perpendicular to the far-field **c**-director (Figs. 1 and 2). We will discuss

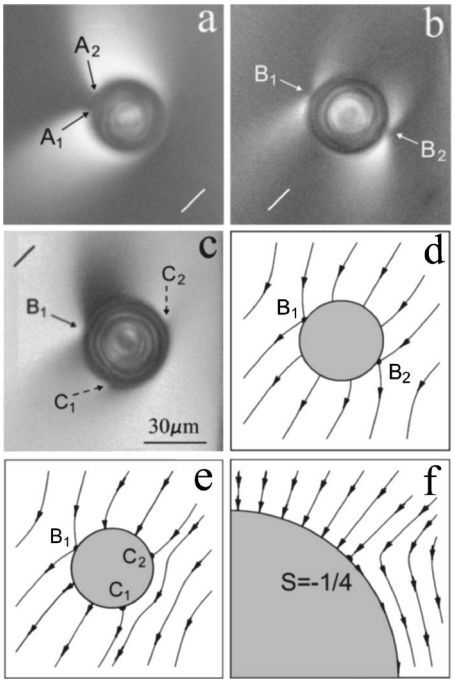


FIG. 7. Formation of quadrupolar configuration near the droplets in 9BSMHOB membranes. (a) The mixed configuration with two topological defects $A_1$ and $A_2$ ($S=-1/2$), $T=105.6$ °C. (b) The quadrupolar configuration with two $B_1$ and $B_2$ defects ($S=-1/2$) on the opposite sides of the droplet, $T=105.9$ °C. The transition from the mixed to the quadrupolar configuration occurs at $T=105.8$ °C: each of $A_1$ and $A_2$ defects (a) splits in two $S=-1/4$ defects, which move along the droplet boundary in opposite directions and adjoining form a quadrupolar structure with two $S=-1/2$ defects ($B_1$ and $B_2$) on the opposite sides of the droplet. (c) An intermediate state ($T=105.8$ °C): two $S=-1/4$ defects already joined to form an $S=-1/2$ defect ($B_1$), but two other defects with $S=-1/4$ (shown by the dotted arrows, $C_1$ and $C_2$) continue to move along the droplet boundary. Lines show the **c**-director orientation in the black ($a$,$b$) and bright ($c$) regions of the photos (DRLM). A schematic representation of the **c**-director field in the quadrupolar configuration (d) with two $S=-1/2$ defects and in the intermediate state (e) with one $S=-1/2$ topological defect ($B_1$) and two $S=-1/4$ topological defects ($C_1$ and $C_2$). A schematic representation of the **c**-director field near the $S=-1/4$ topological defect on an enlarged scale (f).

in detail the formation of radial surface orientation for the case of quadrupolar configuration (Fig. 7). As pointed out in Sec. III A, the dipolar configuration transforms into a configuration with two $S=-1/2$ topological defects [$A_1$ and $A_2$ in Fig. 7(a)]. Further heating induces the transformation of topological defects and the **c**-director field never observed earlier: each $S=-1/2$ defect splits into two $S=-1/4$ defects that move in opposite directions along the droplet boundary. Two of the four $S=-1/4$ defects born by $A_1$ and $A_2$ defects merge into a new $S=-1/2$ defect denoted $B_1$. Two other $S=-1/4$ defects adjoin on the opposite side of the droplet forming the $B_2$ defect with $S=-1/2$ [Fig. 7(b)]. So, a quadrupolar configuration with two $S=-1/2$ topological defects is formed. The motion of the $S=-1/4$ topological defects turns the **c**-director by 90° on the droplet boundary. In the quadrupolar configuration the orientation of the **c**-director on

the droplet boundary is radial [Fig. 7(d)]. Figure 7(c) shows the intermediate state when two $S=-1/4$ defects have already joined in the $B_1$ ($S=-1/2$) defect, but two other $S=-1/4$ defects ($C_1$ and $C_2$) still move to the opposite side of the droplet. A schematic representation of the **c**-director configuration near the droplet with one $S=-1/2$ topological defect and two $S=-1/4$ topological defects is shown in Fig. 7(e). In Fig. 7(f), we show the $S=-1/4$ defect on an enlarged scale. The boundary condition is radial on one side from the $S=-1/4$ defect and tangential on the other side from the $S=-1/4$ defect. The final configuration [Fig. 7(b)] is quadrupolar with a texture near the droplet typical for the quadrupolar configuration. Chains disjointed during the reorientation of the **c**-director field form again under the influence of the quadrupole-quadrupole interparticle interaction.

When the dipolar structure with radial anchoring is formed [Figs. 5(d) and 6] only one of the two $S=-1/2$ defects [Fig. 5(c)] splits in two $S=-1/4$ defects. They move along the droplet boundary in opposite directions and form a dipolar structure with radial orientation of the **c**-director on the droplet boundary. The transformation of the topological defects and the **c**-director field is reversible, i.e., under cooling the quadrupolar and dipolar droplets with radial **c**-director orientation transform to dipolar droplets with planar orientation on the inclusion boundary.

Upon heating above the bulk transition temperature $T_C$ the thinning transitions in membranes take place [28]. At thinning the director orientation on the inclusion boundary changes back from radial to planar. This is in accordance with general membrane behavior since in membranes structural transitions are shifted to high temperatures with decreasing membrane thickness [15]. The reorientation of the **c**-director on the inclusion boundary is also shifted to higher temperatures in thinner membranes. Transformations of the **c**-director orientation at thinning as well as thinning transitions themselves are irreversible. After thinning at further heating the **c**-director reorientation again takes place and the boundary conditions become radial. We observed radial orientation of the **c**-director in membranes thicker than nine layers. In thinner membranes the transition to radial orientation was not observed.

## IV. DISCUSSION

Our experiments show that individual and collective behavior of inclusions in liquid-crystal media is essentially more complex than presumed earlier. The existing theories should be modified considerably not only for the quantitative but even for a qualitative description of the observed phenomena. Complete theoretical understanding of the phase behavior and all observed topological phase transitions is far from a simple task owing to the many relevant degrees of freedom determining the behavior, inherent to all liquid crystals anisotropic and intrinsically nonlinear elasticity, the existence of widely different length scales. These factors make the problem very difficult to treat even numerically. In our paper we shall touch neither of these tricky issues, guided by the prejudice that simple qualitative questions should be addressed first. Thus in this section we shall only note possible reasons for the unusual behavior of the inclusions, surface topological defects, and reorientation of the director field.

A stable configuration of the **c**-director field corresponds to the minimum of the free energy of the membrane with given boundary conditions on the inclusion surface. Usually the free-energy density is taken in the form of quadratic elastic energy of 2D **c**-director field

$$F_{SB} = \frac{1}{2}K_S(\nabla \cdot \mathbf{c})^2 + \frac{1}{2}K_B(\nabla \times \mathbf{c})^2. \tag{2}$$

On the phenomenological level anchoring energy can be described by two basic parameters: the easy-axis direction **e**, and the anchoring potential strength $W$. For our case (ferroelectric Sm$C^*$ membranes) the surface energy can be written as

$$F_2 = F_{SF}(\phi), \tag{3}$$

where $\phi$ is the angle of **c**-director orientation on the droplet boundary. To be specific, we take $\phi=0$ for tangential **c**-director orientation. For ferroelectric membranes, besides two quadratic gradient elastic terms (1) additional terms in the free energy $F$ should be introduced.

$$F_3 = F_S + F_B + F_E + F_L. \tag{4}$$

Two terms $F_S$ and $F_B$ linear over the derivatives of **c** have different physical origin. The second term

$$F_B \propto \lambda_B[\nabla \times \mathbf{c}]_z \tag{5}$$

arises from chirality [30–34]. The $F_S$ term

$$F_S \propto \lambda_S(\nabla \cdot \mathbf{c}) \tag{6}$$

should exist even in nonchiral membranes because in films **c** is a true vector and $\nabla \cdot \mathbf{c}$ is a scalar [35]. Note that if the magnitude of the molecular tilt is uniform, with the result that the projection **c** has constant length (i.e., $|\mathbf{c}|$), then the $F_B$ term (5) is a total derivative that can be reduced to a line integral around the inclusion perimeter. Therefore the $F_B$ contribution in this case can be absorbed into the definition of the inclusion anchoring energy $F_2$ (3). In polar membranes splay of polarization (bend in elastic distortion) gives rise to space charges and electric contribution $F_E$ to the free energy [14,36]. Due to this term, in ferroelectric membranes droplets interact not only through topological but also electric charges [29]. $F_L$ is the standard Landau expansion of the free energy in powers of **c**,

$$F_L = \frac{1}{2}a|c|^2 + \frac{1}{4}b|c|^4 + \frac{1}{6}d|c|^6 + \mathbf{h} \cdot \mathbf{c}, \tag{7}$$

where **h** is the parameter representing the strength of the anisotropic field associated with molecular tilt. For ferroelectric systems with a polar vector order parameter **p** with a number of components $n>1$ the Landau free-energy expansion over this order parameter, besides the conventional terms (which are similar to those in Eq. (7) up to replacement $\mathbf{c} \rightarrow \mathbf{p}$) a new third-order term is allowed, which is chiral by its nature [like the $F_B$ energy (5)]

$$F_{ch} \propto [\mathbf{p}^2 \nabla \cdot \mathbf{p} - (\mathbf{p} \cdot \nabla)\mathbf{p}^2]. \quad (8)$$

Note that symmetry under time reversal would always result in such a term vanishing in a magnetic system, and in addition it will vanish in a centrosymmetric system. Change of the modulus of **c** in membranes may be essential in our case since we performed most of the experiments at high temperature $T > T_C$. Note also that $\lambda_B$ depends on $|\mathbf{c}|^2$, which couples variations of modulus **c** with variations in the **c**-director orientation.

Tangential orientation of the **c**-director on the boundary of smectic islands and droplets is observed at low temperature. We may guess that $F_{SF}(\phi)$ dominates and has a minimum at $\phi=0$. So, reconstruction of the **c**-director field described in Sec. III A is due to the change of the other terms with temperature. The linear over gradients terms (5), (6), and (8) favor only one direction of **c**-field rotation. Depending on the signs of $\lambda_B$ and $\lambda_S$ it may be either clockwise or counterclockwise tangential rotation of the **c**-director ($\lambda_B$ term), inward or outward **c**-director rotation near the droplets ($\lambda_S$ term) [37].

Competition of $F_S$ and $F_B$ terms in the free energy selects the direction of **c**-field rotation near the inclusion. Above $T_C$ the profile of the order parameter across the membrane becomes essentially inhomogeneous. This leads to a sufficient increase of the $\lambda_S$ term in the free energy. The favorable direction of **c** rotation may change with temperature due to the change of the relative contribution in the energy $F_B$ and $F_S$ terms above $T_C$ and the corresponding contribution of the electrostatic energy $F_E$.

At low temperature the $F_{SF}(\phi)$ term dictates the **c**-director reconstruction with conservation of planar **c**-director orientation on the droplet boundary. However, contrary to the $F_{SF}(\phi)$ term, the elastic and electrostatic $F_E$ terms favor radial orientation of the **c**-director. In ferroelectric membranes $K_B > K_S$ [36], so the elastic energy near the droplet is minimal for radial orientation. Moreover, the radial orientation (splay deformation of the **c**-director) does not give rise to space charges. In our opinion the competition between the surface $F_{SF}(\phi)$ term and the elastic and electrostatic terms leads to the formation of radial surface orientation at high temperature.

The overall treatment above can be generalized to more realistic models, with the same conceptual ingredients, albeit at the expense of a rapidly increasing complexity. For instance, the interaction between inclusions and defect structures require more specific and detailed investigation. Indeed, any object injected into the liquid-crystal film produces in the liquid-crystal medium distortions whose dimensions considerably exceed its own size. Another injected inclusion if it enters the distorted region will interact effectively with the first one. What is relevant is that this interaction is long ranged and noncentral, and has both attractive and repulsive parts depending on mutual positions and orientations of the inclusions. The isotropic forces should cause hexagonal ordering, while, for example, for the dipolar symmetry the attraction forms chainlike structures. If the director field is uniform far from the particle, the total topological charge of the whole system is zero. Thus topological considerations imply that for sufficiently strong anchoring an additional defect (or defects depending on the topological charges) must be created in the liquid-crystal medium. In this case the **c**-director orientation field becomes singular and within a small region $l$ around the defect the module of the order parameter vanishes. The core energy of the defect arises from this small region. One can use a simple ansatz for the order parameter module profile

$$c = c_{eq}[1 - \exp(-r/l)], \quad (9)$$

where $c_{eq}$ is the modulus of the order parameter $|\mathbf{c}|$ far from the defect. Introducing this trial function into the free-energy expansion (4) and minimizing over $l$ one can estimate the variational parameter $l$, which is proportional to the Sm$C$ ordering correlation length $\xi$,

$$l \propto |S|\xi, \quad (10)$$

where $S$ is the defect charge. If $l$ is smaller than the other characteristic lengths of the system, one can safely use the continuous energy expansion (4) to compare the energies of various configurations. However, the energy is well defined outside the core region only, and the total free energy should be estimated by adding to it the core energy, which scales as

$$F_{core} \propto S^2 K. \quad (11)$$

As a result of the attractive component of the interactions, defects aggregate around the inclusions. They can be aggregated either on the inclusion surface or at a certain small but finite distance from the surface.

## V. CONCLUSION

Up to now, in smectic membranes different configurations of the **c**-director field were observed: dipolar, quadrupolar, and mixed. It was presumed that the configuration of the **c**-director field is constant for a given liquid-crystal compound and inclusion. Our study shows that in polar membranes the **c**-director configuration is strongly temperature dependent resulting from the rearrangement of the topological defects on the droplet boundary. The number and strength of defects may change with temperature.

(i) The splitting of the $-1$ defect into two $-1/2$ defects and their motion along the droplet boundary change the tangential orientation of the **c**-director by an angle $\pi$. After director reorientation the defects recombine again into a $-1$ defect.

(ii) The transition between tangential and radial orientation results from splitting of $-1/2$ defects into four $-1/4$ defects, their motion on droplet boundary, and recombination into a pair of $-1/2$ defects.

(iii) The collective behavior of droplets changes significantly with **c**-director reorientation. The experimental conditions leading to reorientation effects are well reproduced.

Our results can be used also in another way, as a technique to estimate the surface anchoring strength. This estimation of the anchoring energy is related to the development of theory describing the present results. Our observations open the way for manipulation of both isolated inclusions

and structures formed by inclusions.

The unusual behavior of surface topological defects and the **c**-director field is not described by existing theories. They are based mainly on quadratic elasticity of the liquid-crystal media and do not account for peculiarities of polar liquid crystals. Further experimental and theoretical studies are necessary for revealing the nature of the observed phenomena.

## ACKNOWLEDGMENTS

This work was supported in part by the Russian Foundation for Basic Research Grant No. 05-02-16675, INTAS Grant No. 06-1000014-6462, and by the Russian Science Support Foundation. We are grateful to L. Lejcek for helpful discussions.

[1] P. Poulin, H. Stark, T. C. Lubensky, and D. A. Weitz, Science **275**, 1770 (1997).
[2] T. C. Lubensky, D. Pettey, N. Currier, and H. Stark, Phys. Rev. E **57**, 610 (1998).
[3] P. Poulin and D. A. Weitz, Phys. Rev. E **57**, 626 (1998).
[4] J.-C. Loudet, P. Barois, and P. Poulin, Nature (London) **407**, 611 (2000).
[5] P. Poulin, V. Cabuil, and D. A. Weitz, Phys. Rev. Lett. **79**, 4862 (1997).
[6] P. Cluzeau, P. Poulin, G. Joly, and H. T. Nguyen, Phys. Rev. E **63**, 031702 (2001).
[7] P. Cluzeau, G. Joly, H. T. Nguyen, and V. K. Dolganov, Pis'ma Zh. Eksp. Teor. Fiz. **75**, 573, (2002) [JETP Lett. **75**, 482 (2002)].
[8] P. Cluzeau, G. Joly, H. T. Nguyen, and V. K. Dolganov, Pis'ma Zh. Eksp. Teor. Fiz. **76**, 411, (2002) [JETP Lett. **76**, 351 (2002)].
[9] P. V. Dolganov, E. I. Demikhov, B. M. Bolotin, V. K. Dolganov, and K. Krohn, Eur. Phys. J. E **12**, 593 (2003).
[10] C. Völtz and R. Stannarius, Phys. Rev. E **70**, 061702 (2004).
[11] C. Völtz and R. Stannarius, Phys. Rev. E **72**, 011705 (2005).
[12] P. V. Dolganov and V. K. Dolganov, Phys. Rev. E **73**, 041706 (2006).
[13] V. G. Nazarenko, A. B. Nych, and B. I. Lev, Phys. Rev. Lett. **87**, 075504 (2001).
[14] C. Y. Young, R. Pindak, N. A. Clark, and R. B. Meyer, Phys. Rev. Lett. **40**, 773 (1978).
[15] W. H. de Jeu, B. I. Ostrovskii, and A. N. Shalaginov, Rev. Mod. Phys. **75**, 181 (2003).
[16] P. G. de Gennes and J. Prost, *The Physics of Liquid Crystals*, 2nd ed. (Clarendon Press, Oxford, 1993).
[17] D. Pettey, T. C. Lubensky, and D. Link, Liq. Cryst. **25**, 5 (1998).
[18] C. Bohley and R. Stannarius, Eur. Phys. J. E **20**, 299 (2006).
[19] J.-B. Lee, D. Konovalov, and R. B. Meyer, Phys. Rev. E **73**, 051705 (2006).
[20] E. M. Terentjev, Phys. Rev. E **51**, 1330 (1995).
[21] H. Stark, Eur. Phys. J. B **10**, 311 (1999); Phys. Rep. **351**, 387 (2001).
[22] H. Stark, Phys. Rev. E **66**, 032701 (2002).
[23] S. Grollau, N. L. Abbott, and J. J. de Pablo, Phys. Rev. E **67**, 011702 (2003).
[24] J. Fukuda, M. Yoneya, and H. Yokoyama, Eur. Phys. J. E **13**, 87 (2004).
[25] C. Völtz, Y. Maeda, Y. Tabe, and H. Yokoyama, Phys. Rev. Lett. **97**, 227801 (2006).
[26] P. Cluzeau, M. Ismaili, A. Annakar, M. Foulon, A. Babeau, and H. T. Nguyen, Mol. Cryst. Liq. Cryst. Sci. Technol., Sect. A **362**, 185 (2001).
[27] D. R. Link, G. Natale, R. Shao, N. A. Clark, E. Korblova, and D. M. Walba, Science **84**, 3665 (1999).
[28] T. Stoebe, P. Mach, and C. C. Huang, Phys. Rev. Lett. **73**, 1384 (1994).
[29] P. V. Dolganov, H. T. Nguyen, G. Joly, V. K. Dolganov, and P. Cluzeau, Europhys. Lett. **76**, 250 (2006).
[30] D. Blankschtein and R. M. Hornreich, Phys. Rev. B **32**, 3214 (1985).
[31] S. A. Langer and J. P. Sethna, Phys. Rev. A **34**, 5035 (1986).
[32] G. A. Hinshaw and R. G. Petschek, Phys. Rev. A **39**, 5914 (1989).
[33] J. V. Selinger, Z. G. Wang, R. F. Bruinsma, and C. M. Knobler, Phys. Rev. Lett. **70**, 1139 (1993).
[34] R. D. Kamien and J. V. Selinger, J. Phys.: Condens. Matter **13**, R1 (2001).
[35] R. B. Meyer and P. S. Pershan, Solid State Commun. **13**, 989 (1973).
[36] D. R. Link, N. Chattham, J. E. Maclennan, and N. A. Clark, Phys. Rev. E **71**, 021704 (2005).
[37] I. Kraus and R. B. Meyer, Phys. Rev. Lett. **82**, 3815 (1999).